34th Annual International Conference of the IEEE EMBS
San Diego, California USA, 28 August - 1 September, 2012

Automatic Brain Tumor Extraction from T1-weighted Coronal MRI Using Fast Bounding Box and Dynamic Snake

Tao Xu and Mrinal Mandal, *Senior Member, IEEE*

Abstract— **Brain tumor segmentation from MRI data is an important but challenging task. This paper presents an efficient and fully automatic brain tumor segmentation technique. The proposed technique includes a fuzzy C-means (FCM) based preprocessing to enhance the quality of T1-weighted coronal MR images, a fast bounding box (FBB) detection algorithm to locate a rectangle around tumor, and a new dynamic snake using modified Hausdorff distance (MHD) for the final tumor extraction.**

I. Introduction

Since Magnetic Resonance Imaging (MRI) can provide better contrast between different soft tissues of human brain compared to Computed Tomography (CT), it is the most common image modality used in clinical practice for brain tumor diagnosis. Typically, radiologist performs manual delineation of tumor region and imparts the details to neurologist, which is very time-consuming due to the huge volume of images [1]. Thus, computer-aided brain tumor segmentation from MRI data has been an active area of research in recent years. However, automating this process is still a challenging problem due to the high variation in appearance of tumor tissues among different patients.

Most of the existing techniques proposed for brain tumor segmentation are not fully automatic due to expert-required model training or user-guided initialization or other user interaction. For example, Kaus et al. [2] proposed an adaptive template–moderated classification algorithm to segment brain MRI slices into five different tissue classes (background, skin, brain, ventricles, and tumor). Prastawa et al [3] proposed a brain tumor segmentation framework based on Expectation Maximization (EM) algorithm and outlier detection, where tumors are considered as outliers of the Gaussian model. These techniques detect tumor regions using a registered brain atlas as a model for healthy brains. Except for the professional work of atlas generation, large deformation of tumors requires significant modification of the atlas which may lead to poor results. Much more flexible techniques without priori information were developed to overcome these problems. Phillips et al. [4] first applied the fuzzy C-means (FCM) clustering to segment brain tumors. One of its drawbacks is that human interaction is required. Liu et al. [5] adapted the fuzzy connectedness framework for tumor segmentation with limited user interaction. However, the fuzzy model works well only for hyper intensity (fully enhanced) tumors and exhibit poor performance on detecting non-enhanced tumors. Active contours such as snake, and level-set achieve popularity in brain tumor segmentation because of its great potential for 3D medical image segmentation. Lefohn et al. [6] applied a level-set implementation using GPUs but user interactive for initialization is needed. Ho et al. [7] incorporated region competition into level-set algorithm for brain tumor segmentation to overcome the initialization and weak edge leakage problems. But the technique has high computational cost. Wang et al. [8-9] proposed a dynamic external force, Fluid Vector Flow (FVF), for snake model and extended to 3D tumor segmentation. However, their initialization whether manual [8] or atlas-based [9] suffers similar problems.

In this paper, we propose a fast and fully automatic brain tumor segmentation technique based on snake model, which can be divided into three major steps. First, a FCM-based preprocessing is applied to increase the quality of T1 coronal MR images. Second, the fast bounding box (FBB) method using symmetry[10] is adopted to detect the bounding box of brain tumor. Finally, using the bounding box as the initial contour, a dynamic snake with new external force is proposed for the tumor extraction. Snake model is more preferable than level-set as: 1) level-set is much slower than snake in virtue of higher dimensional embedding; 2) level-set produces more false alarms due to the multiple objects capturing ability.

The rest of this paper is organized as follows: Section II provides a brief related background work. In Section III, the proposed method is described in detail. The experimental results for brain tumor segmentation are presented in Section IV followed by the conclusions in Section V.

II. Related Work

A. Fast Bounding Box(FBB) Using Symmetry[10]

The FBB is an approximate segmentation technique which explores the symmetry of brain structure to locate a bounding box around the tumor. Given a 2D MR image, which is a T1C (T1 after injecting a contrast agent) MR slice in [10], the FBB casts the problem as a change detection problem. The algorithm can be described as follows:

1) Image halving based on brain structure symmetry

The MR image first needs to be divided into two parts: one half of the brain acts as a reference image *R*, and the other half as a test image *I*. After the skull contour is detected by Otsu's thresholding [10], the geometrical axis of symmetry of the skull is then applied to halve the image.

2) Bounding box detection based on Bhattacharya coefficient (BC)

The FBB finds the region of abnormality *D* which is an axis-parallel rectangle by considering both horizontal and

Manuscript received on March 15th, 2012. Tao Xu and Mrinal Mandal (Corresponding Author) are with the department of Electrical and Computer Engineering, University of Alberta , Edmonton, AB, T6G 2V4, Canada. (e-mail: tx1@ualberta.ca, mmandal@ualberta.ca).

vertical score functions defined by the Bhattacharya coefficient (*BC*).

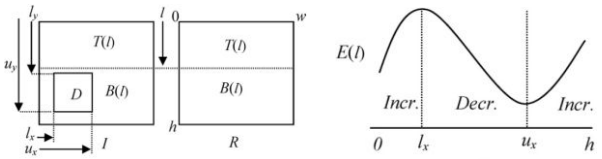

(a) (b)

Fig. 1. (a) Finding bounding box *D* from test image *I* using reference image *R*.. (b) Score function plot observed in vertical sweep.

As illustrated in Fig. 1(a), the rectangle region $D=[l_x,u_x]\times[l_y,u_y]$ represents the region of change containing a tumor. $T(l)$ and $B(l)$ are respectively the top and bottom subrectangles of the image, divided at a distance l from the top of the image. FBB then finds the best l_y and u_y values in a vertical sweep (moving the dotted line vertically) using a score function:

$$E(l) = BC(P_I^{T(l)}, P_R^{T(l)}) - BC(P_I^{B(l)}, P_R^{B(l)}) \qquad (1)$$

where $P_I^{T(l)}$ denotes the normalized intensity histogram of the region $T(l)$ in the test image. $P_R^{T(l)}$, $P_I^{B(l)}$ and $P_R^{B(l)}$ are defined accordingly. $BC(a,b)=\sum_i \sqrt{a(i)b(i)} \in [0,1]$ denotes the Bhattacharya coefficient between two normalized histograms $a(i)$ and $b(i)$, with i indicating a histogram bin.

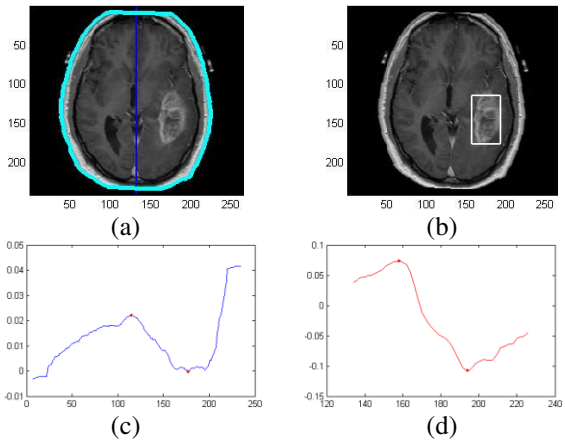

(a) (b) (c) (d)

Fig. 2. Locating brain tumor from T1C MR slice using FBB. (a) Skull boundary and line of symmetry; (b) Detected bounding box; (c) Vertical score plot; (d) Horizontal score plot

Based on three assumptions: 1) the intensity histogram of *D* is very dissimilar from the intensity histogram of the reference image; 2) the region of the test image outside *D* is very similar to the intensity histogram of the reference image; 3) intensity histograms are independent of *l*, Saha et al. [10] established the "increasing-decreasing-increasing" nature of $E(l)$ (shown in Fig. 1(b)). Since the increasing and decreasing segments meet at $l=l_x$ and $l=u_x$, the lower and upper bounds of *D*, respectively, the upper and lower bounds for *D* can be located quickly from the vertical score plot. Similar procedure will be done to find the left and right bounds. Fig. 2 is an example of the FBB method applied in a T1C MR slice.

B. Dynamic Snake

In snake model [11], the curve evolves through the image plane to minimize the following energy functional:

$$E_{snake} = \int_0^1 \left[\frac{1}{2}(\alpha |v'(s)|^2 + \beta |v''(s)|^2) + E_{ext}(v(s)) \right] ds \qquad (2)$$

where $v(s)$ represents a parameterized curve, α and β are weighting parameters. E_{ext} denotes the external energy related to image features, such as edges. The solution to Eq. (2) can be treated as a force balance equation [12]:

$$F_{int}(v) + F_{ext}(v) = 0 \qquad (3)$$

where $F_{int}(v) = \alpha v''(s) - \beta v''''(s)$ is the internal force constraining contour's smoothness, and $F_{ext}(v) = -\nabla E_{ext}(v)$ is the external force attracting contour toward image features.

Efforts made to improve the performance by designing different external forces can be generally classified as static forces and dynamic forces. The static forces calculated from the image remain unchanged while the dynamic forces dependent on the snake change as the snake deforms [12]. Recent improvements have been made by adding certain dynamic force term into the static external force to overcome the saddle points problem, such as snake with Dirichlet boundary conditions (DBC) [13] and FVF [8-9].

1) Fluid Vector Flow (FVF)[8]

The external forces in FVF can be treated as combination of two components, static force F_{static} and dynamic force $F_{dynamic}$, where $F_{static} = \chi(\nabla I(x,y))$ is just the normalized gradient of a given image *I*. (χ and ∇ are the normalized and gradient operators, respectively.) The key idea of $F_{dynamic}$ is to add a directional distance force which can be generated in two sequential steps:

First, in the vector flow initialization step, $F_{dynamic} = (\delta\cos\phi, \delta\sin\phi)$, where $\delta = \pm 1$ controls snake's inward or outward direction, and ϕ is the angle between a point (x, y) (except the points on the object boundary) and the center point of the contour. $(\cos\phi, \sin\phi)$ is actually the normalized Euclidean distance force between them.

Second, in the FVF computation step, $F_{dynamic} = (\delta\chi(x-x_q), \delta\chi(y-y_q))$, where the normalized distance part is changed to the distance between a point (x, y) (except the points on the object boundary) and the point (x_q, y_q) picked up from the object boundary (named as control point). The control point will move along the object boundary during each iteration, that is why it is called as fluid vector flow.

III. PROPOSED METHOD

In this section, we propose an automatic brain tumor segmentation technique whose schematic is shown in Fig. 3. The proposed technique has three steps: a fuzzy C-means (FCM) based preprocessing, fast bounding box (FBB) based initialization, and a modified Hausdorff distance based dynamic snake (MHD-DS) for tumor extraction. Details of these steps are presented below.

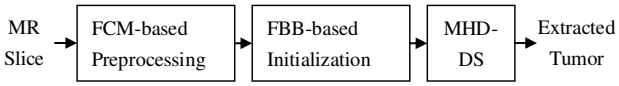

Fig. 3. Schematic of the proposed technique.

A. FCM based Preprocessing

Since the test datasets are coronal view of MRI scans, the image symmetry is poorer than axial view due to more non-brain anatomical structures involved. To satisfy the FBB's assumptions, a subimage from top to 2/3 of the original height is empirically selected as the brain region in our preliminary test (See Fig. 4(a)).

Next, we apply FCM [4] to cluster the MR subimage into three classes considering relative structures in different intensity levels. Figs. 4(b), (c) show an example of FCM clustering results, and the tumor is greatly enhanced in class 3.

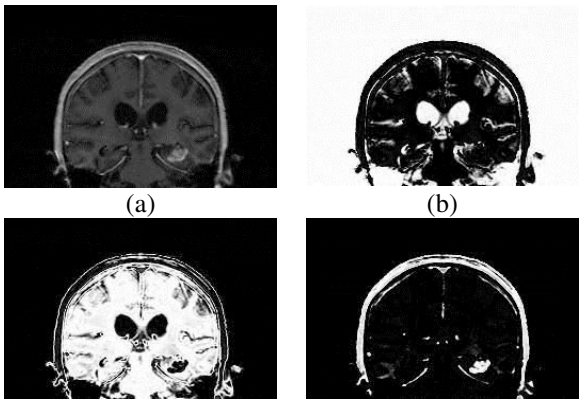

Fig. 4. (a) Original T1-weighted coronal MR slice. (b-d) Clustering results using FCM.

B. FBB based Initialization

In this step, the FBB [10] is adopted to find single tumor's bounding box in the preprocessed subimage. This bounding box will be used as the initialization contour for the next step's snake model based segmentation. Since the bounding box is sometimes inside the tumor, we expand the segmentation area to a larger rectangle region (block image) with the same centroid and axis-parallel to the detected bounding box. In our experiment, this block image is fixed as 64×64 pixels. Fig. 5 shows the bounding box and the block image, respectively.

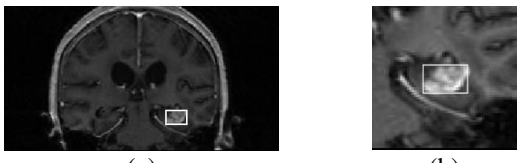

Fig. 5. (a) FBB detection based on Fig. 4(d); (b) Block image with initial contour for the next MHD-DS step.

C. MHD-DS for Tumor Extraction

In this step, we propose a new dynamic snake to extract the tumor by addressing the limitations of FVF. First, the external force of FVF can be consolidated as follows:

$$F_{FVF} = F_{static} + F_{dynamic} = \chi(\nabla I(x,y) + (1-f)\delta\chi(\nabla d(x,y))) \quad (4)$$

where $f = |\nabla I(x,y)|$ is the binary boundary map, and d is the Euclidean distance between a point (x, y) (except the points on the object boundary) and the control point (either center point of the contour or the points on the object boundary). The term $(1-f)$ makes the dynamic distance force zero for those points reaching to the object boundary.

Although the FVF enlarges the capturing range into the whole image and solve the saddle points problem, it has two drawbacks including edge leakage caused by distance force term and inefficiency of control point selection. Figs. 6(a)-(c) shows an example of FVF's failure to large edge gaps. The first drawback can easily be handled by changing the F_{static} from normalized image gradient to other static external force which overcomes the edge leakage, e.g. GVF [12] and BVF [14]. Fig. 6(d) is the result of using normalized BVF as F_{static} in Eq. (4).

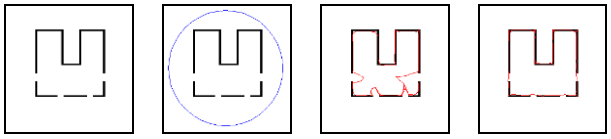

Fig. 6. (a) Object with two edge gaps (b) The initial contour (c) Result of FVF (d) Result of FVF with static force such as BVF.

As for the second drawback, our strategy is to consider the point which contributes more to the distance between snake contour and object boundary. For instance, in Fig. 7 where solid contour stands for the snake contour at current iteration, and dotted contour is the object boundary, the control point sequentially selected along the object boundary in FVF treats all the object boundary points equally. It is actually not true, and in this case point o3 should be given more weights to attract the snake. By treating this problem as two point sets matching, an appropriate control point can be selected using MHD which has been shown to provide good matching performance [16].

Finally, the external force of our proposed dynamic snake is concluded as follows:

$$F_{MHD-DS} = \chi(F_{BVF} + (1-f)\delta\chi(\nabla d'(x,y))) \quad (5)$$

where d' is the Euclidean distance between any point (x, y) on the image plane and the new defined control point.

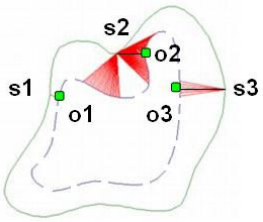

Fig. 7. An example of control point selection. s1-s3, o1-o3 are points on the snake contour and object boundary, respectively.

IV. Experimental Results

A. Materials

The experimental dataset has been obtained from the public Internet Brain Segmentation Repository (IBSR) [15] which contains six T1-weighted Coronal MRI scans of two tumor patients over a period of time. From each scan, 7-10 slices with brain tumors were selected for the segmentation test. Expert's manual delineation of tumor in each slice is treated as the ground truth. The platform for all the tests is Matlab 2007b on a Intel Pentium 4 CPU 2.8G Hz with 2G RAM computer.

B. Segmentation Performance Evaluation

1) FBB detection accuracy

The FBB detection performance is evaluated by the missing rate (MR), which is defined as follows:

$$MR = \frac{\#\text{ of Bounding Boxes Excluding Tumor}}{\text{Total \# of Tumor Slices}} \times 100\% \quad (6)$$

Table I shows the result of FBB with and without FCM preprocessing.

TABLE I. FBB Detection Evaluation

	FBB Without Preprocessing	**FBB With Preprocessing**
Total # of Tumor Slices	50	50
MR	50%	16%

2) MHD-DS segmentation accuracy

The segmentation performance of the proposed MHD-DS technique was evaluated using Tanimoto metric (TM) [8], which is defined as:

$$TM = \frac{\left\| R_c \cap R_g \right\|}{\left\| R_c \cup R_g \right\|} \times 100\% \quad (7)$$

where R_c denotes the region enclosed by the contour generated using segmentation techniques; R_g denotes the tumor region enclosed by the ground truth. The evaluation results is shown in Table II, by comparing with other dynamic snakes. It is observed that our proposed MHD-DS achieves the best accuracy and robustness. Considering the computational cost, both DBC and MHD-DS are efficient for real-time practice. Several segmentation results are shown in Fig. 8.

TABLE II. Segmentation Evaluation

	DBC	**FVF**	**MHD-DS**
TM (Avg.±Std.)	56.7%± 12.4%	62.6± 9.2%	69.6± 7.1%
Time-cost (sec)	0.95	3.65	1.56

V. Conclusion

In this paper, a computer-aided fully automatic brain tumor segmentation technique is proposed for T1-weighted Coronal MRI data without any priori information. It provides lower missing rate and higher segmentation accuracy comparing to existing techniques. Future work may include decreasing the MR for snake's initialization, and extending the technique into 3D application.

Acknowledgment

The authors would like to thank Dr. Nilanjan Ray, University of Alberta, for sharing the source code of FBB. They would also like to acknowledge Massachusetts General Hospital for the brain tumor MRI images [15].

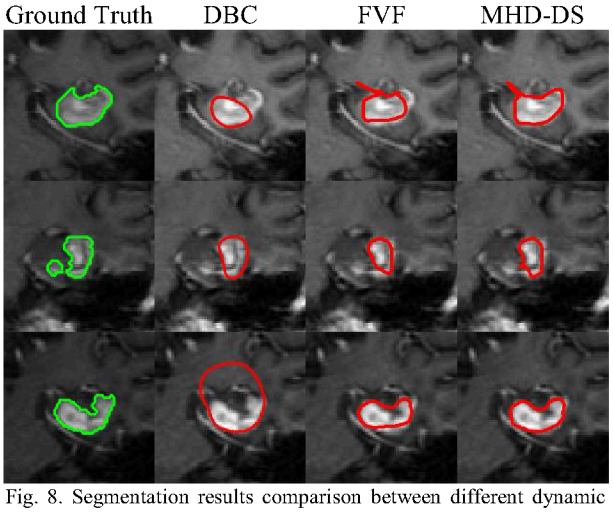

Fig. 8. Segmentation results comparison between different dynamic snakes in the same block images.

References

[1] K. Brindle, "New approaches for imaging tumour responses to treatment," *Nature Reviews Cancer*, 2008, 8:94–107.

[2] M. Kaus, S. K. Warfield, et al, "Automated segmentation of MRI of brain tumors," *Radiology*, 2001, 218(2):586–91.

[3] M. Prastawa, E. Bullitt, S. Ho, and G. Gerig, "A brain tumor segmentation framework based on outlier detection," *Med. Image Anal.*, 2004, 8(3):275–283.

[4] W.E. Phillips, R.P. Velthuizen, et al, "Application of fuzzy c-means segmentation technique for tissue differentiation in MR images of a hemorrhagic glioblastoma multiforme," *MRI*, 1995, 13(2): 277–290.

[5] J. Liu, J.K. Udupa, et al, "A system for brain tumor volume estimation via MR imaging and fuzzy connectedness," *CMIG* 2005, 29(1):21–34.

[6] A. Lefohn, J. Cates, and R. Whitaker, "Interactive, GPU-based level sets for 3D brain tumor segmentation," *MICCAI*, 2003.

[7] S. Ho, E. Bullitt, and G. Gerig, "Level set evolution with region competition: Automatic 3-D segmentation of brain tumors," in *Proc. ICPR*, 2002, 532–535.

[8] T. Wang, I. Cheng and A. Basu, "Fluid vector flow and applications in brain tumor segmentation", *IEEE TBME*, 2009, 56(3):781-789.

[9] T. Wang, I. Cheng, and A. Basu, "Fully automatic brain tumor segmentation using a normalized Gaussian Bayesian Classifier and 3D Fluid Vector Flow", in *Proc. ICIP*, 2010, 2553-2556.

[10] B.N. Saha, N. Ray, et al, "Quick detection of brain tumors and edemas: a bounding box method using symmetry," *CMIG*, 2012, 36(2):95-107.

[11] M. Kass, A.Witkin, and D. Terzopoulus, "Snakes: Active Contour Model," *IJCV*, 1988, 1(4):321–331.

[12] C. Xu and J. Prince, "Snakes, Shapes, and Gradient Vector Flow," *IEEE TIP*, 1998, 7(3):359–369.

[13] R. Shen, I. Cheng, and A. Basu, "A hybrid knowledge-guided detection technique for screening of infectious pulmonary tuberculosis from chest radiographs," *IEEE TBME*, 2010, 57(11):2646-2656.

[14] K.W. Sum and P.Y.S. Cheung, "Boundary vector field for parametric active contours," *PR*, 2007, 40(6):1635–1645.

[15] Image Dadaset: http://www.cma.mgh.harvard.edu/ibsr/. (Oct., 2011).

[16] M.P. Dubuisson and A.K. Jain, "A modified Hausdorff distance for object matching," *ICPR*, 1994, 566–568